Primljen / Received: 9.6.2020.
Ispravljen / Corrected: 25.7.2022.
Prihvaćen / Accepted: 3.1.2024.
Dostupno online / Available online: 10.2.2024.

Periodic structure as seismic barriers

Author:

Assoc.Prof. **Julin Wang**, PhD. CE
Shanxi Architectural College, China
Institute of Building Structures
wangjl_tj@163.com
Corresponding author

Research Paper

Julin Wang

Periodic structure as seismic barriers

Some seismic barriers are periodic structures with the characteristic of frequency band gaps (BGs) similar to sonic crystals, which can protect buildings from damage caused by earthquakes. Their working idea is to arrange periodic structures in the foundation around the buildings you want to protect, and the seismic wave is blocked outside the buildings when the frequencies of seismic waves exactly fall in the frequency BGs of the seismic barriers. Based on sonic crystal, a periodic structure is first presented here, which not only can be utilised as seismic barriers but also has a large internal space to provide the possibility for other functions such as civil air defence construction, line access, etc. The frequency BGs of the presented structure are determined by the spectral element method, and the influence of geometrical parameters and the number of unit cells on the frequency BGs is analysed. Numerical calculation confirms that the proposed structure can effectively isolate some seismic waves.

Key words:
seismic waves, vibration isolation, frequency band gaps, spectral element method, periodic structures

Prethodno priopćenje

Julin Wang

Konstrukcija periodički ponavljajućih oblika i svojstava kao seizmička barijera

Neke su seizmičke barijere zapravo konstrukcije periodički ponavljajućih oblika i svojstava karakterizirane pojavom jaza u frekvencijskom pojasu (eng. *frequency band gaps* - BG) nalik zvučnim kristalima, koji mogu zaštititi zgrade od oštećenja uzrokovanih potresima. Ideja je postavljanje takvih konstrukcija kao temelja oko zgrada koje se žele zaštititi, a seizmički val blokira se izvan zgrada kada su frekvencije seizmičkih valova unutar frekvencijskog jaza seizmičkih barijera. U radu je predstavljena konstrukcija ponavljajućih oblika i svojstava, koja ne samo da se može primijeniti kao seizmička barijera, već također ima velik unutarnji prostor za druge funkcije kao što je izgradnja civilne protuzračne obrane, mrežni pristup itd. Jaz frekvencijskoga pojasa prikazane konstrukcije određen je metodom spektralnih elemenata te je analiziran utjecaj geometrijskih parametara i broja jediničnih ćelija na njega. Numerički proračun potvrđuje da predložena konstrukcija može učinkovito izolirati određene seizmičke valove.

Ključne riječi:
seizmički valovi, vibracijska izolacija, jaz frekvencijskog pojasa, metoda spektralnih elemenata, konstrukcije periodički ponavljajućih oblika i svojstava

1. Introduction

Earthquakes cause huge property damage and deprive many people of their lives, and approximately two earthquakes occur per minute on the earth [1]. The conventional seismic isolation methods include passive control, active control, and hybrid control techniques [2-6], and generally, these techniques often have little effect on large earthquakes [7].

A periodic structure made of phononic crystals and locally resonant metamaterials acts as seismic wave barriers to greatly attenuate the amplitude of seismic waves before they reach the protected target [8-12]. This approach has two advantages: a) it can protect distributed areas rather than just a single building; b) it does not change the natural frequency of the protected structures. Liu et al. [13] discovered sonic crystals with unconventional properties, such as the frequency BGs, i.e., frequency ranges within which waves cannot propagate. The periodic structures are arranged in the foundation in an array around the structures [14] to be protected, as illustrated in Figure 1; thus, the buildings of interest can be protected from earthquake damage [15].

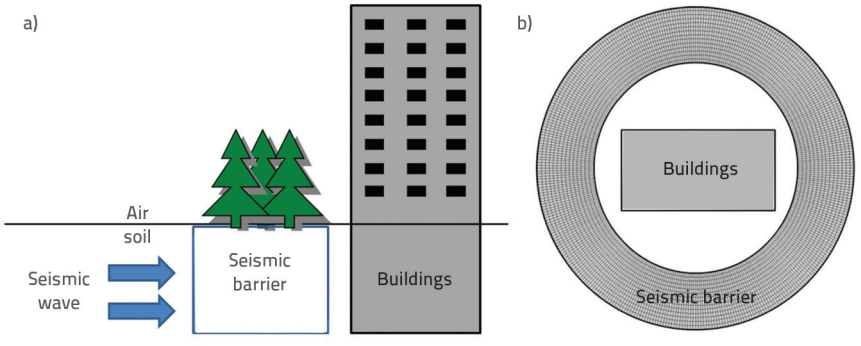

Figure 1. Seismic barriers: a) Side view; b) Plan view

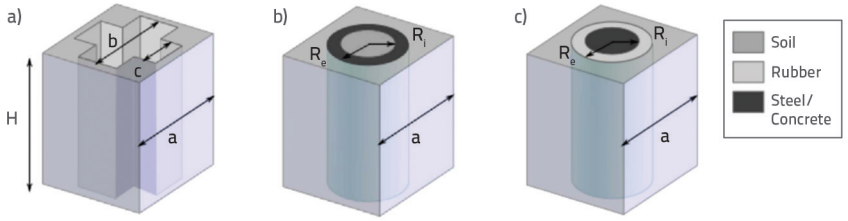

Figure 2. Three kinds of unit cells: a) Cross-like cavity; b) Hollow cylinder; c) Coated cylinder

Some scholars have done a lot of work on seismic barriers. Meseguer and Holgado [16] discovered the existence of frequency BGs for the first time via experiments. Finocchio et al. [17] presented a seismic barrier composed of a set of mass-in-mass systems, which can filter S-wave. Marco et al. [7] proposed three different types of unit cells, as illustrated in Figure 2 and numerically analysed both surface and guided waves. The result confirmed that the seismic barriers composed of the three kinds of unit cells can block the two waves.

The wavelength of different seismic waves varies widely, ranging from several kilometres to as short as tens of metres. The width of the seismic barrier surrounding buildings is closely related to the wavelength of seismic waves. The longer the seismic wave, the larger the width of the seismic barrier required (SANG and MUKUNDA, 2012). The materials for seismic barriers, whether concrete, steel, or other materials, are expensive owing to the huge number of unit cells. In addition, seismic barriers cover a large area. Based on the above two aspects, seismic barriers are expected to have more functions. A periodic structure made of concrete and rubber is presented here. The structure has the characteristic of frequency BGs, which can be utilised as a seismic barrier, and a large internal space, as demonstrated in Figure 3, which provides the possibility for other functions such as civil air defence, line access, etc.

A periodic structure is composed of several unit cells that are the same in terms of structure and materials. The spectral element method (SEM) can treat a unit cell as a spectral unit, which greatly reduces the number of units, thereby reducing the degrees of freedom of the entire periodic structure [18, 19]. In addition, the same high-precision frequency domain results can be obtained by the SEM as by the finite element method [20]. Therefore, the spectral element method is employed to analyse the frequency BGs of the proposed periodic structure, and then the factors affecting the frequency BGs are deeply considered in detail.

2. Basic theory of presented periodic structure

The periodic structure proposed here is arranged in a square array under the ground around the buildings to be protected, as illustrated in Figure 3. Each row contains N unit cells made of two materials along the x^g direction of the global coordinate (x^g, y^g, z^g), as demonstrated in Figure 4.

It is assumed that each plate of a unit cell has the properties of elasticity, homogeneity and isotropy. Each plate of a unit cell has small deformations, and the lateral shear deformation is negligible; hence, they belong to the Kirchhoff plates.

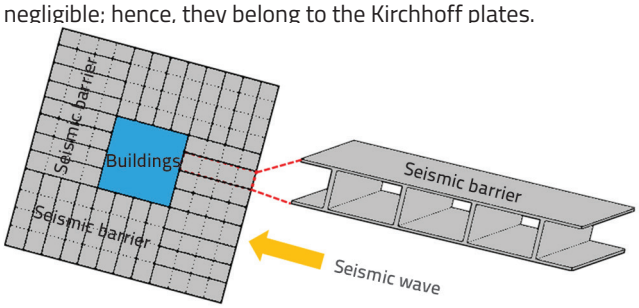

Figure 3. Top view of proposed seismic barrier

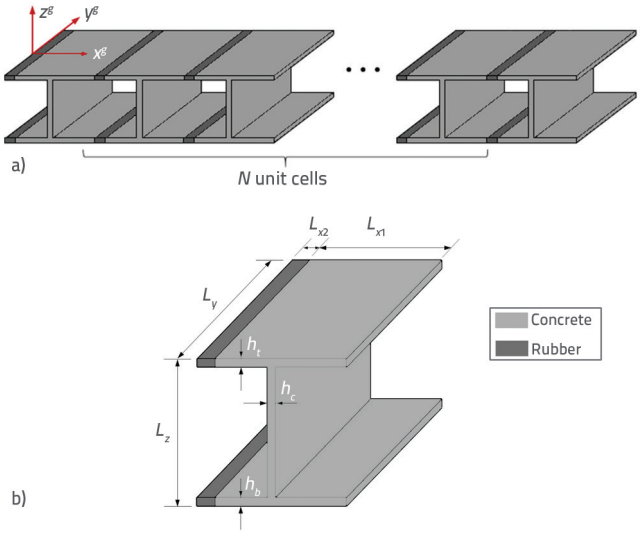

Figure 4. Presented periodic structure: a) Combination of N unit cells; b) One unit cell

Within a small deformation range, the deformation of the plates can be decoupled into in-plane and out-of-plane components. Before constructing the motion equations of the periodic structure in the global coordinate system, the spectral dynamic equations of plates are established in the local coordinate system.

2.1. Out-of-plane vibration

Figure 5 represents a simple-supported plate with opposite sides in the local coordinate system (x, y, z), which is *L* long, *b* wide, and *h* thick.

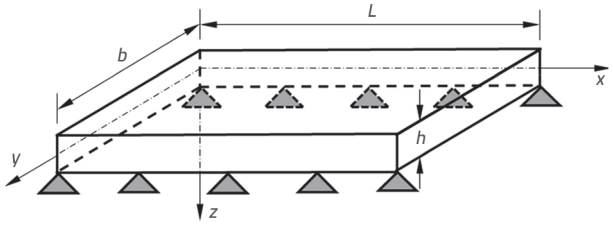

Figure 5. Simple-supported plate with opposite sides

The bending vibration equation of out-of-plate for Kirchhoff plates is, Eq. (1):

$$D\nabla^4 w + \rho h \frac{\partial^2 w}{\partial t^2} = 0 \tag{1}$$

where $D = Eh^3/[12(1-\mu^2)]$is the bending rigidity of the plate; w is the displacement in the z direction; ρ is the mass density; μ is the Poisson's ratio; E is the Young's Modulus.
Figure 6 presents the internal forces of the plate, and the shear force and bending moment are given by Eq. (2):

$$\begin{cases} Q_x = -D\left(\dfrac{\partial^3 w}{\partial x^3} + (2-\mu)\dfrac{\partial^3 w}{\partial x \partial y^2}\right) \\ M_x = -D\left(\dfrac{\partial^2 w}{\partial x^2} + \mu\dfrac{\partial^2 w}{\partial y^2}\right) \\ Q_y = -D\left(\dfrac{\partial^3 w}{\partial y^3} + (2-\mu)\dfrac{\partial^3 w}{\partial y \partial x^2}\right) \\ M_y = -D\left(\dfrac{\partial^2 w}{\partial y^2} + \mu\dfrac{\partial^2 w}{\partial x^2}\right) \end{cases} \tag{2}$$

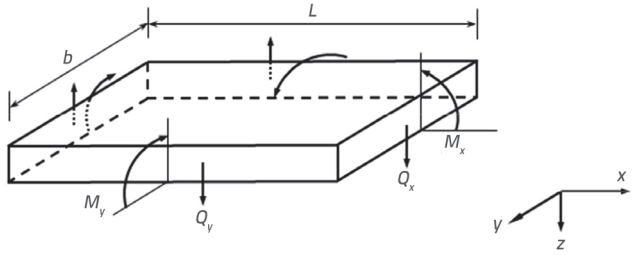

Figure 6. Schematic of plate with positive internal forces

The spectral stiffness equation of out-of-plane for Kirchhoff plate element is Eq. (3), according to [21]:

$$\mathbf{S}_{out}\left(k_y,\omega_n\right)\mathbf{d}_{out}\left(k_y,\omega_n\right) = \mathbf{f}_{out}\left(k_y,\omega_n\right) \tag{3}$$

where k_y = (mπ/6), (m = 1, 2, 3, ...) s the wave number along the y direction; m is the mode number; w_n is the circular frequency; S_{out}, d_{out} and f_{out} are the spectral stiffness matrix, the displacement vector in the wavenumber domain and the internal force vector in the wavenumber domain, respectively, which can be expressed as

$$\begin{cases} \mathbf{S}_{out}\left(k_y,\omega_n\right) = \mathbf{G}_{out}\left(k_y,\omega_n\right)\boldsymbol{\Phi}_{out}^{-1}\left(k_y,\omega_n\right) \\ \mathbf{d}_{out}\left(k_y,\omega_n\right) = \boldsymbol{\Phi}_{out}\left(k_y,\omega_n\right)\mathbf{A} \\ \mathbf{f}_{out}\left(k_y,\omega_n\right) = \mathbf{G}_{out}\left(k_y,\omega_n\right)\mathbf{A} \end{cases} \tag{4}$$

where $A = [A_1\ A_2\ A_3\ A_4]^T$, A_1, A_2, A_3 and A_4 are four unknown coefficients, G_{out} and Φ_{out} are given by Eq. (5)

$$\begin{cases} \mathbf{G}_{out} = -D\left[g_{ij}\right], \quad (i,j = 1,\ 2,\ 3,\ 4) \\ \quad g_{1j} = -p_j^3 + (2-\mu)k_y^2 p_j\ ; \qquad g_{2j} = -p_j^2 + \mu k_y^2 \\ \quad g_{3j} = p_j^3 e^{p_j L} - (2-\mu)k_y^2 p_j e^{p_j L}\ ; \quad g_{4j} = -p_j^2 e^{p_j L} + \mu k_y^2 e^{p_j L} \\ \boldsymbol{\Phi}_{out} = \begin{bmatrix} 1 & 1 & 1 & 1 \\ -p_1 & -p_2 & -p_3 & -p_4 \\ e^{p_1 L} & e^{p_2 L} & e^{p_3 L} & e^{p_4 L} \\ -p_1 e^{p_1 L} & -p_2 e^{p_2 L} & -p_3 e^{p_3 L} & -p_4 e^{p_4 L} \end{bmatrix} \end{cases} \tag{5}$$

Where $p_1 = \sqrt{\omega_n\sqrt{\rho h/D} + k_y^2}$, $p_2 = \sqrt{-\omega_n\sqrt{\rho h/D} + k_y^2}$,

$p_3 = -\sqrt{\omega_n\sqrt{\rho h/D} + k_y^2}$ and $p_4 = -\sqrt{-\omega_n\sqrt{\rho h/D} + k_y^2}$

2.2. In-plane vibration

The motion equations of in-plane vibration for Kirchhoff plates are given by Eq. (6):

$$\begin{cases} \dfrac{\partial^2 u}{\partial x^2}+\dfrac{1-\mu}{2}\dfrac{\partial^2 u}{\partial y^2}+\dfrac{1+\mu}{2}\dfrac{\partial^2 v}{\partial x\partial y}-\dfrac{\rho(1-\mu^2)}{E}\dfrac{\partial^2 u}{\partial t^2}=0 \\ \dfrac{\partial^2 v}{\partial x^2}+\dfrac{1-\mu}{2}\dfrac{\partial^2 v}{\partial y^2}+\dfrac{1+\mu}{2}\dfrac{\partial^2 u}{\partial x\partial y}-\dfrac{\rho(1-\mu^2)}{E}\dfrac{\partial^2 v}{\partial t^2}=0 \end{cases} \tag{6}$$

where u and v represent the in-plane longitudinal and in-plane shear displacements in the x and y directions, respectively.
The spectral stiffness equation of in-plate vibration for the Kirchhoff plate is given by Eq. (7) according [22]:

$$S_{in}\left(k_y,\omega_n\right)d_{in}\left(k_y,\omega_n\right)=f_{in}\left(k_y,\omega_n\right) \tag{7}$$

where S_{in}, d_{in} and f_{in} are the spectral stiffness matrix, the displacement vector in the wavenumber domain and the internal force vector in the wavenumber domain, respectively, which can be expressed as, Eq. (8):

$$\begin{cases} \mathbf{S}_{in}\left(k_y,\omega_n\right)=\mathbf{G}_{in}\left(k_y,\omega_n\right)\mathbf{\Phi}_{in}^{-1}\left(k_y,\omega_n\right) \\ \mathbf{d}_{in}\left(k_y,\omega_n\right)=\mathbf{\Phi}_{in}\left(k_y,\omega_n\right)\mathbf{C} \\ \mathbf{f}_{in}\left(k_y,\omega_n\right)=\mathbf{G}_{in}\left(k_y,\omega_n\right)\mathbf{C} \end{cases} \tag{8}$$

where $C=[C_1C_2C_3C_4]^T$ is the coefficient vector, C_1, C_2, C_3 and C_4 are four unknown coefficients, G_{in} and Φ_{in} are given by Eq. (9):

$$\mathbf{G}_{in}=\begin{bmatrix} -\alpha\left(\delta_1^2-\mu k_y^2\right) & -\alpha\left(\delta_2^2-\mu k_y^2\right) & -\alpha\left(\delta_3^2-\mu k_y^2\right) & -\alpha\left(\delta_4^2-\mu k_y^2\right) \\ -2\beta k_y\delta_1 & -2\beta k_y\delta_2 & -\beta\left(k_y^2+\delta_3^2\right) & -\beta\left(k_y^2+\delta_4^2\right) \\ \alpha\left(\delta_1^2-\mu k_y^2\right)e^{\delta_1 L} & \alpha\left(\delta_2^2-\mu k_y^2\right)e^{\delta_2 L} & \alpha(1-\mu)k_y\delta_3 e^{\delta_3 L} & \alpha(1-\mu)k_y\lambda_4 e^{\delta_4 L} \\ 2\beta k_y\delta_1 e^{\delta_1 L} & 2\beta k_y\delta_2 e^{\delta_2 L} & \beta\left(k_y^2+\delta_3^2\right)e^{\delta_3 L} & \beta\left(k_y^2+\delta_4^2\right)e^{\delta_4 L} \end{bmatrix} \tag{9}$$

$$\mathbf{\Phi}_{in}=\begin{bmatrix} \delta_1 & \delta_2 & k_y & k_y \\ k_y & k_y & \delta_3 & \delta_4 \\ \delta_1 e^{\delta_1 L} & \delta_2 e^{\delta_2 L} & k_y e^{\delta_3 L} & k_y e^{\delta_4 L} \\ k_y e^{\delta_1 L} & k_y e^{\delta_2 L} & \delta_3 e^{\delta_3 L} & \delta_4 e^{\delta_4 L} \end{bmatrix} \tag{10}$$

where $\alpha = Eh/(1-\mu^2)$; $\beta = Eh/[2(1+\mu)]$; $\delta_{1,2}=\pm\sqrt{k_y^2-k_L^2}$;

$\delta_{3,4}=\pm\sqrt{k_y^2-k_S^2}$; $k_L=\omega\sqrt{\rho(1-\mu^2)/E}$ and $k_s=\omega\sqrt{2\rho(1+\mu)/E}$

are the wave numbers of the in-plane longitudinal wave and shear wave.

2.3. Spectral motion equation of presented periodic structure

Based on Eqs. 3 and 7, we can get the spectral stiffness equation of both in-plane and out-of-plane vibrations for the Kirchhoff plate, which is given by Eq. (11)

$$S_p\left(k_y,\omega_n\right)d_p\left(k_y,\omega_n\right)=f_p\left(k_y,\omega_n\right) \tag{11}$$

where $\mathbf{d}_p$ and $\mathbf{f}_p$ are the plate's nodal displacement vector and nodal force vector, respectively; $\mathbf{S}_p$ is the spectral stiffness matrix of the plates, including in-plane and out-of-plane vibration components.
Eqs. 3 and 7 are derived from the local coordinate system, and the vibration of each plate of the periodic structure needs to be described in the global coordinate system. The relationship of the plate between the local and global coordinate system is demonstrated in Figure 7, which is given by Eq. (12):

$$\begin{Bmatrix} x \\ y \\ z \\ \theta \end{Bmatrix}=\begin{bmatrix} \cos\varphi & 0 & \sin\varphi & 0 \\ 0 & 1 & 0 & 0 \\ -\sin\varphi & 0 & \cos\varphi & 0 \\ 0 & 0 & 0 & 1 \end{bmatrix}\begin{Bmatrix} x^g \\ y^g \\ z^g \\ \theta^g \end{Bmatrix} \tag{12}$$

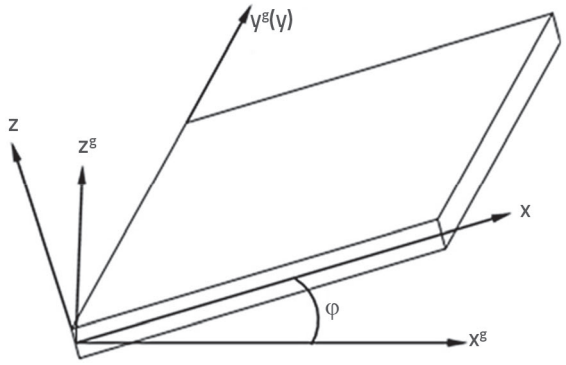

Figure 7. Plate element in local and global coordinate systems

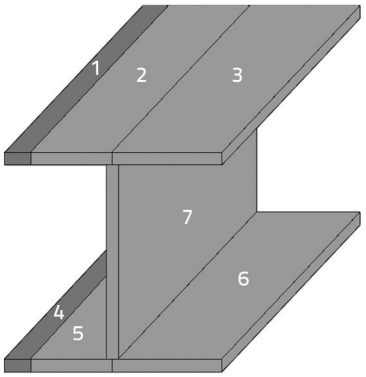

Figure 8. Unit cell divided into seven spectral plate elements

A unit cell can be divided into seven spectral plate elements, as illustrated in Figure 8. Eq. 11 is obtained in the local coordinate system. The relationships of the displacement and force vectors between the global coordinate system and the local one can be given as (13)

$$\begin{cases} d_p=T_r d_p^g \\ f_p=T_r f_p^g \end{cases} \tag{13}$$

where:
d_p^g and f_p^g are the displacement and force vectors in the global coordinate system,

$\tau_r = \begin{bmatrix} \Lambda & 0 \\ 0 & \Lambda \end{bmatrix}$ is the transformation matrix which is equal to

$$\Lambda = \begin{bmatrix} \cos\varphi & 0 & \sin\varphi & 0 \\ 0 & 1 & 0 & 0 \\ -\sin\varphi & 0 & \cos\varphi & 0 \\ 0 & 0 & 0 & 1 \end{bmatrix} \begin{Bmatrix} x^g \\ y^g \\ z^g \\ \theta^g \end{Bmatrix} \quad (14)$$

Substituting Eq. (13) into Eq. (11), the spectral stiffness matrix of the plate in the global coordinate can be obtained.

$$\mathbf{S}_p^g = \mathbf{T}_r^T \mathbf{S}_p \mathbf{T}_r \quad (15)$$

where S_p^g is the spectral stiffness matrix of the plate in the global coordinate system.
The spectral motion equation of the periodic structure can be derived by assembling the plates in the global coordinate system.

$$\mathbf{S}(k_y, \omega_n)\mathbf{d}(k_y, \omega_n) = \mathbf{f}(k_y, \omega_n) \quad (16)$$

where $\mathbf{S}(k_y, w_n)$ is the spectral stiffness matrix of the periodic structure in the global coordinate system; $\mathbf{d}(k_y, w_n)$ and $\mathbf{f}(k_y, w_n)$ are the displacement and the force vector of the periodic structure, respectively.
By solving Eq. (16), the dynamic responses of the periodic structure can be calculated, and then the frequency BGs of the structure analysed.

3. Analysis and discussion

In this section, the frequency responses of the presented periodic structure are calculated by the SEM, and the influences of some parameters on the frequency BGs of the structure are investigated in detail. The materials of the unit cell are concrete (with Young's modulus E_c = 30 GPa, Poisson's ratio m_c = 0.25, mass density ρ_c= 2500 kg/m^3) and rubber (with Young's modulus E_r = 120 kPa, Poisson's ratio μ_r = 0.47, mass density ρ_r= 1300 kg/m^3), respectively. The external disturbance force $F = F_0 e^{iwt}$ is applied on the left boundary of the periodic structure, and the action point is the centroid of the cross-section of the structure, where F_0 = 12 kN. The force F acts along the xg axis and points to this structure. To better illustrate the presented periodic structure to attenuate waves in the frequency domain effectively, we define frequency response function (FRF) as $20\log(d_j/d_i)$, where d_i and d_j denote the displacements in the x^g direction of the action point and the centroid of the right edge of the structure, respectively. In the calculations, we consider unit cells under the assumption of free–free boundary conditions applied to the top and bottom surfaces. Other boundary conditions [22] will be considered in future studies.

3.1. Effects of geometrical parameters on frequency BGs

To study the effects of geometrical parameters on the frequency BGs, the number of unit cells in each row is 4, as illustrated in Figure 3, and remains unchanged in this section.

3.1.1. Thickness of plates

Three cases are considered and analysed, and the corresponding geometrical parameters are presented in Table 1. The irreducible Brillouin zone ΓXM is considered, where Γ = (0, 0), X = (Π/L_x, 0), M = (Π/L_x, Π/L_x).

Table 1. Geometric parameters with different thickness of plates (unit: mm)

Case	L_{x1}	L_{x2}	L_y	L_z	h_t	h_c	h_b
1	5700	300	6000	6000	100	100	100
2					200	200	200
3					300	300	300

Figs. 9 and 10 present the frequency response of the periodic structure due to the change in the thickness of the plates.

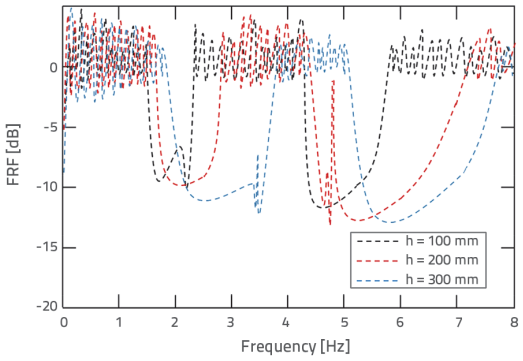

Figure 9. Frequency responses with different plate thicknesses

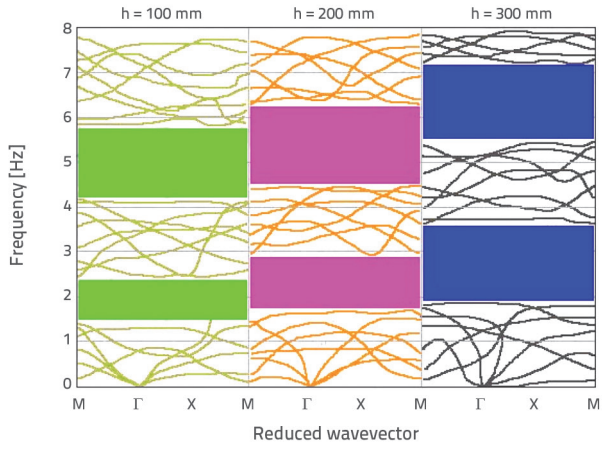

Figure 10. Dispersion diagrams for different plate thicknesses

There are two frequency BGs (1.46–2.35 Hz) and (4.23–5.74 Hz) for Case 1, (1.73–2.87 Hz) and (4.52–6.23 Hz) for Case 2,

(1.90–3.56 Hz) and (5.38–7.22 Hz) for Case 3, respectively. This indicates that the periodic structure has the frequency BGs. As the thickness of the plate increases, the BGs widen and shift to higher frequencies, which implies that appropriately increasing the thickness of the plates is conducive to improving the effect of vibration isolation of the periodic structure.

3.1.2. Height-to-width radio of unit cell: L_z/L_y

Three cases are considered to analyse the effect of Lz/Ly on the frequency BGs. The geometrical properties of a unit cell are listed in Table 2.

Table 2. Geometric parameters with different height-to-width radio (unit: mm)

Case	L_{x1}	L_{x2}	L_y	L_z	h_t	h_c	h_b
1	5700	300	6000	3000	200	200	200
2				6000			
3				12000			

Figure 11 indicates that the height of a unit cell plays an essential role in forming the frequency BGs. The width of the BGs is inversely related to the value of L_z/L_y; that is, as L_z/L_y increases, the width of the frequency BGs is reduced, and the ability to suppress wave propagation is impaired. The fundamental reason for the phenomenon is that more and more high-order plate modes appear with the value of L_z/L_y increasing [23]. Therefore, for smaller radios of Lz/Ly, the frequency BGs are generated because of the 'folding' of the lowest frequency bands. For larger values of L_z/L_y, as the ratio L_z/L_y increases, higher order modes appear, the cut-off frequency increases, and the frequency BGs eventually disappear (Marco et al., 2016).

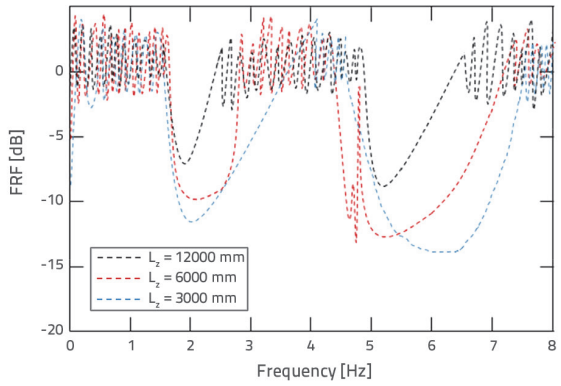

Figure 11. Frequency responses with different height-to-width radios

3.1.3. L_{x1} and L_{x2}

Because the material of the upper flange with the width L_{x2} of the unit cells is rubber, to ensure the stability of the part in the plane and outside, the maximum value of L_{x2} is 350 mm. Seven cases are studied, and the geometrical properties of a unit cell are presented in Table 3. Figure 12 illustrates the frequency BGs in the seven cases.

The figure indicates the width variation of the two frequency BGs. As L_{x2} increases, the BG sizes are enlarged. This occurs because of the decrease in the stiffness of the upper flange with the width L_{x2}. In Case 1, three frequency BGs appear, which is narrower than the other cases. Under the premise of ensuring structural stability, the shielding performance of the periodic structure can be improved by appropriately increasing the value of L_{x2}.

Table 3. Geometric parameters with different values of L_{x1} and L_{x2} (unit: mm)

Case	L_{x1}	L_{x2}	L_y	L_z	h_t	h_c	h_b
1	5950	50	6000	6000	200	200	200
2	5900	100					
3	5850	150					
4	5800	200					
5	5750	250					
6	5700	300					
7	5650	350					

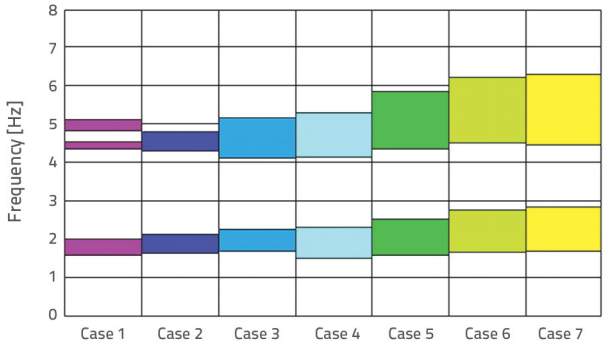

Figure 12. Complete BGs indicated in colour regions of seven cases

3.2. Effects of number N of unit cells in each row on frequency BGs

In the section, the frequency BGs of the proposed periodic structure are also analysed for different numbers N of unit cells in each row. In the calculation, the values of N are 0, 1, 2, 3, 4, 5, 6 and 7, respectively. The geometrical properties of a unit cell are listed in Table 4.

Table 4. Geometric parameters with different numbers N of unit cells (unit: mm)

L_{x1}	L_{x2}	L_y	L_z	h_t	h_c	h_b
5700	300	6000	600	200	200	200

Figure 13 reports the maximum displacement at the centroid of the right edge of the structure to the different number N of unit cells in each row for wave frequencies centred in the frequency BGs (at 3.75 and 5 Hz). The displacements are normalised with respect to the maximum one obtained as the number N of unit cells equals zero. The figure reveals that the wave amplitude decays exponentially as the number of unit cells increases.

Considering economic factors, generally, the value of N is 4 or 5. In this case, seismic waves are much weakened.

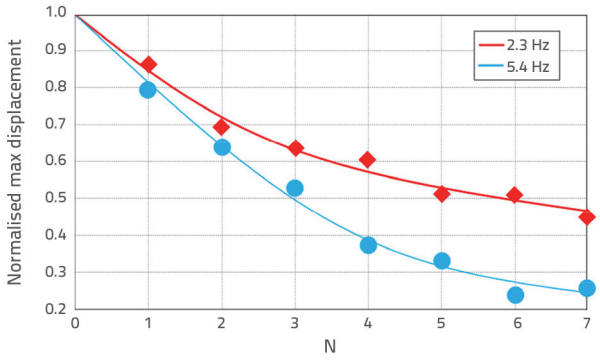

Figure 13. Normalised displacement to number N of unit cells for 2.3 Hz and 5.4 Hz

4. Conclusion

Here, a periodic structure as seismic barriers is proposed and proved to be effective in attenuating waves produced by the external disturbance force defined for this case study. The calculation results have confirmed that the unit cells' aspect ratio and plate thickness largely affect the size and boundaries of the frequency BGs. Owing to the wide frequency distribution of earthquakes, we cannot block all earthquakes from the protected buildings. However, we can make appropriate adjustments to the geometric parameters such that the natural frequencies of the buildings fit into the gaps to avoid the risk of structural resonance. In addition, the structure has a large space, which provides the necessary possibility for realising other functions. Herein, body waves are not numerically analysed, and the soil dissipation effects are not considered, which will be carried out in the following research.

Acknowledgements

The author would like to acknowledge the support of Dr. Tang Shougao, Tongji University, and Professor Hou Xinlu, Taiyuan University of Technology, for their invaluable support and encouragement.

REFERENCES

[1] Bilham, R.: Lessons from the Haiti earthquake, Nature, 463 (2010), pp. 878-879, https://doi.org/10.1038/ 463878a

[2] Spencer, B., Nagarajaiah, S.: State of the art of structural control, Struct. Eng., 129 (2003) 7, pp. 845-856, https://doi.org/10.1061/(ASCE)0733-9445(2003)129:7(845)

[3] Tamahloult, M., Tiliouine, B.: 3D nonlinear seismic analysis and design of base-isolated buildings under near field ground motions, GRAĐEVINAR, 75 (2023) 5, pp. 483-493, https://doi.org/ https://doi.org/10.14256/JCE.3548.2022

[4] Başgöze, A., Güncü, A.: Determining the regional disaster risk analysis of buildings in Erzincan, GRAĐEVINAR, 75 (2023) 3, pp. 257-272, https://doi.org/10.14256/JCE.3436.2021

[5] Mertol, H.C., Tunc, G., Akis, T.: A site survey of damaged RC buildings in İzmir after the Aegean Sea earthquake on October 30, 2020, GRAĐEVINAR, 75 (2023) 5, pp. 451-470, https://doi.org/10.14256/JCE.3343.2021

[6] Halkijević, I., Vouk, D., Posavčić, H., Mostečak, H.: Damage assessment of water supply networks due to seismic events using vulnerability functions, GRAĐEVINAR, 73 (2021) 7, pp. 737-749, https://doi.org/10.14256/JCE.3185.2021

[7] Miniaci, M., Krushynska, A., Bosia, F., Pugno, N.M.: Large scale mechanical metamaterials as seismic shields, New J. Phys, 18 (2016) 083041, pp. 1-14, https://doi.org/10.1088/ 1367-2630/18/8/083041

[8] Ho, K.M., Cheng, C.K., Yang, Z.: Broadband locally resonant sonic shields, Appl Phys Lett, 83 (2003) 26, pp. 5566-5568, https://doi.org/10.1063/1.1637152

[9] Zhang, S., Hua, J., Cheng, J.C.: Experimental and theoretical evidence for the existence of broad forbidden gaps in the three-component composite, Chin Phys Lett, 20 (2003) 8, pp. 1303-1305, https://doi.org/10.1088/0256-307X/ 20/8/335

[10] Miniaci, M., Marzani, A., Testoni, N., Marchi, L.D.: Complete band gaps in a polyvinyl chloride (PVC) phononic plate with cross-like holes: numerical design and experimental verification, Ultrasonics, 56 (2015), pp. 251-259, https://doi.org/10.1016/j.ultras.2014.07.016

[11] Mazzotti, M., Miniaci, M., Bartoli, I.: Band structure analysis of leaky Bloch waves in 2D phononic crystal plates, Ultrasonics, 74 (2017), pp. 140-143, https://doi.org/10.1016/j.ultras.2016.10.006

[12] Pennec, Y., Vasseur, J.O., Bahram, D.R., Dobrzyński, L., Deymier, P.A.: Two dimensional phononic crystals: examples and applications, Surface Science Reports, 65 (2010) 8, pp. 229-291, https://doi.org/10.1016/j.surfrep.2010. 08,002

[13] Zhengyou, L., Xixiang, Z., Yiwei, M., Zhu, Y.Y., Zhiyu, Y., Chan, C.T., Ping, S.: Locally Resonant Sonic Materials, SCIENCE, 289 (2000) 5485, pp. 1734-1736, https://doi.org/10.1126/science.289.5485.1734

[14] Sang, H.K., Mukunda, P.: Seismic Waveguide of Metamaterials, Modern Physics Letters B, 26 (2012) 17, pp. 1-8, https://doi.org/10.1142/S0217984912501059

[15] Krodel, S., Thomé, N., Daraio, C.: Wide band-gap seismic metastructures, Extreme Mech. Lett., 4 (2015), pp. 111-117, https://doi.org/10.1016/j.eml.2015.05.004

[16] Meseguer, F., Holgado, M.: Two-dimensional elastic bandgap crystal to attenuate surface waves, Lightwave Technol., 17 (1999), pp. 2196-2201, https://doi.org/10.1109/50.803011

[17] Finocchio, G., Casablanca, O., Ricciardi, G., Alibrandi, U.: Seismic metamaterials based on isochronous mechanical oscillators, Applied Physics Letters, 104 (2014), pp. 1919031-5, https://doi.org/10.1063/1.4876961

[19] Komatitsch, D., Tromp, J.: Introduction to the spectral element method for three-dimensional seismic wave propagation, Geophysical Journal International, 139 (1999) 3, pp. 806-822, https://doi.org/10.1046/j.1365-246x. 1999.00967.x

[10] Kudela, P., Żak, A., Krawczuk, M., Ostachowicz, W.: Modelling of wave propagation in composite plates using the time domain spectral element method, Journal of Sound and Vibration, 302 (2007), pp. 728-754, https://doi.org/10.1016/ j.jsv.2006.12.016

[20] Lee, U., Kim, D., Park, I.: Dynamic modeling and analysis of the PZT-bonded composite Timoshenko beams: Spectral element method, Journal of Sound and Vibration, 332 (2013) 6, pp. 1585-1609, https://doi.org/10.1016/ j.jsv.2012.06.020

[21] Zhijing, W., Fengming, L., Yize, W.: Study on vibration characteristics in periodic plate structures using the spectral element method, Acta Mechanica, 224 (2013) 5, pp. 1089-1101.

[22] Miniaci, M., Kherraz, N., Cröenne, C., Mazzotti, M., Morvaridi, M., Gliozzi, A.S., Onorato,M., Bosia, F., Pugno, N.M.: Hierarchical large-scale elastic metamaterials for passive seismic wave, mitigation, EPJ Appl. Metamat, 14 (2021) 8, pp. 1-8, https://doi.org/10.1051/epjam/2021009

[23] Khelif, A., Aoubiza, B., Mohammadi, S., Adibi, A., Laude, V.: Complete band gaps in two-dimensional phononic crystal slabs, Phys. Rev. E, 74 (2006) 466, pp. 101-105, https://doi.org/10.1103/PhysRevE.74.04661